HAL
open science

Phase property identification using inverse homogenization approaches and field measurements

Thang Vo Quoc, Christian Duriez, Yann Monerie, Stéphane Pagano

To cite this version:

Thang Vo Quoc, Christian Duriez, Yann Monerie, Stéphane Pagano. Phase property identification using inverse homogenization approaches and field measurements. PhotoMechanics 2013, May 2013, Montpellier, France. pp.Clé USB. hal-00833322

HAL Id: hal-00833322

https://hal.science/hal-00833322v1

Submitted on 12 Jun 2013

HAL is a multi-disciplinary open access archive for the deposit and dissemination of scientific research documents, whether they are published or not. The documents may come from teaching and research institutions in France or abroad, or from public or private research centers.

L'archive ouverte pluridisciplinaire **HAL**, est destinée au dépôt et à la diffusion de documents scientifiques de niveau recherche, publiés ou non, émanant des établissements d'enseignement et de recherche français ou étrangers, des laboratoires publics ou privés.

PHASE PROPERTY IDENTIFICATION USING INVERSE HOMOGENIZATION APPROACHES AND FIELD MEASUREMENTS

Q.T. Vo[a,b,c], C. Duriez[a,c], Y. Monerie[a,c] and S. Pagano[b,c].
a. Institut de Radioprotection et de Sureté Nucléaire (IRSN), CE Cadarache, BP3-13115 St Paul-Lez-Durance Cedex, France
b. Laboratoire de Mécanique et Génie Civil, CNRS - Université Montpellier 2, case 048, Place Eugène Bataillon, 34095 cedex 5, France
c. Laboratoire de Micromécanique et d'Intégrité des Structures, CNRS - IRSN - Université Montpellier 2
quoc-thang.vo-cnrs@irsn.fr, christian.duriez@irsn.fr, yann.monerie@irsn.fr, stephane.pagano@univ-montp2.fr

ABSTRACT: In this paper, work is focused on two-phase matrix/inclusion composite materials. A simple method is proposed to identify the elastic properties of one phase while the properties of the other phase are assumed to be known. The method is based on both an inverse homogenization scheme and mechanical fields measurements. The originality of the approach rests on the studied scale: the characteristic size of the inclusions is about few tens of microns.
The identification is performed on standard uniaxial tensile tests. First, the accuracy of the method is estimated on 'perfect' mechanical fields coming from numerical simulations for four microstructures: elastic or porous single inclusions having either spherical or cylindrical shape. Second, this accuracy is validated on real mechanical field for two simple microstructures: an elasto-plastic metallic matrix containing a single cylindrical micro void or four cylindrical micro voids arranged in a square pattern. Third, the method is used to identify elastic properties of inclusions with arbitrary shape in an oxidized α-inclusions / β-matrix Zircaloy-4 sample. In all this study, the phases are assumed to have isotropic properties.

1. INTRODUCTION

We aim here to study the mechanical responses of the Zircaloy-4 nuclear fuel claddings at the scale of the microstructure, having undergone micro-structural changes typical of a postulated loss-of-coolant accident (LOCA). After a LOCA, because of oxygen-diffusion in the material, the cladding will have a heterogeneous microstructure consisting of α-phase inclusions (oxygen-enriched) embedded into a β-phase matrix (low-oxygen content) [1]. A tension-compression device has been equipped with a long-focal-length microscope for observation of the test specimen surface during his solicitation. Associated with image analysis by two-dimensional digital image correlation (2D-DIC) [2], this device directly provides full-field in-plane displacement and strain measurements at the scale of the heterogeneities of the studied material (a few micrometers). In the process of preparing the test specimen surface, etching step allows to create patterns (observable by microscope) required for implementation of 2D-DIC [3, 4]. Spherical aberration correction of recorded images is performed beforehand [5], which allows small strain measurements (order of magnitude of 10^{-3}). The main objective of this study is to determine, by an inverse process of a homogenization method, the elastic properties of the unknown phase from the local and macroscopic measurements of strain fields and stresses during a uniaxial tensile test.

The accuracy of the inverse homogenization method is firstly verified on mechanical fields coming from numerical simulations (CAST3M) in the case of inclusions with simple shapes (spherical inclusion and cylindrical inclusion). The numerical data obtained from the modelled uniaxial tensile test allows to avoid the errors of 'experimental' measurements and provide accurate property estimations of unknown phase. The validation by experimental data is performed afterwards on real porous materials containing cylindrical micro voids since the 2D-DIC technique is based on two-dimensional analysis.

2. A MORI-TANAKA-BASED INVERSE HOMOGENIZATION METHOD

We denote by $i=1$ (resp. $i=2$) the matrix phase (resp. the inclusions). Phase i has volume $|V_i|$ (domain V_i) and volume fraction $f_i = |V_i|/|V|$, where V is the representative volume element. For linear elastic media, the volume average of the strain in each phase $\langle\varepsilon\rangle_i$ depends linearly on the overall strain $\varepsilon^{\text{hom}} = \langle\varepsilon\rangle_V$:

$$\langle\varepsilon\rangle_i = \mathbb{A}_i : \varepsilon^{\text{hom}}, \quad \varepsilon^{\text{hom}} = \sum_{i=1}^{2} f_i \langle\varepsilon\rangle_i, \qquad \langle\varepsilon\rangle_i = \frac{1}{|V_i|}\int_{V_i} \varepsilon(\boldsymbol{x})d\boldsymbol{x} \tag{1}$$

where the $\mathbb{A}_i$ are the strain concentration fourth order tensors. In the case of porous inclusions, the last relation reads :

$$\langle\varepsilon\rangle_2 = \frac{1}{|V_2|}\int_{\partial V_2} \frac{1}{2}\left(\boldsymbol{u}(\boldsymbol{x})\otimes\boldsymbol{N} + \boldsymbol{N}\otimes\boldsymbol{u}(\boldsymbol{x})\right)ds \tag{2}$$

where ∂V_2 denotes the boundary of V_2, $\boldsymbol{N}$ is the outer unit vector and $\boldsymbol{u}$ is the displacement flied.

Focussing on the Mori-Tanaka scheme, the strain concentration tensor $\mathbb{A}_i$ reads [6]:

$$\mathbb{A}_1^{\text{MT}} = \left[f_1\mathbb{I} + f_2\left[\mathbb{I} + \mathbb{P}_1 : (\mathbb{C}_2 - \mathbb{C}_1)\right]^{-1}\right]^{-1}, \qquad \mathbb{A}_2^{\text{MT}} = \left[\mathbb{I} + (1-f_2)\,\mathbb{P}_1 : (\mathbb{C}_2 - \mathbb{C}_1)\right]^{-1} \tag{3}$$

where $\mathbb{I}$ is identity of the fourth-order symmetric tensors $\mathbb{I}_{ijkl} = \frac{1}{2}\left(\delta_{ik}\delta_{jl} + \delta_{il}\delta_{jk}\right)$, δ being the Kronecker symbol, $\mathbb{P}_1$ is the fourth-order Hill's tensor [7] depending on the spatial distribution of the inclusions and on the matrix properties, $\mathbb{C}_i$ is the fourth-order stiffness tensor of the phase i (assumed as isotropic in the sequel).

Moreover, we assume an isotropic (resp. an in-plane isotropic) distribution of phases for spherical (resp. cylindrical) inclusions. The elastic stiffness tensor of each phase and the Hill's tensor thus read as follows [6, 8]:

$$\mathbb{C}_i = 3k_i\mathbb{J} + 2\mu_i\mathbb{K}, \quad \mathbb{P}_1 = \frac{1}{3k_1+4\mu_1}\mathbb{J} + \frac{3}{5\mu_1}\frac{k_1+2\mu_1}{3k_1+4\mu_1}\mathbb{K} \quad \text{for spherical inclusions} \tag{4}$$

$$\left.\begin{aligned} \mathbb{C}_i &= \left(k_i + \frac{4\mu_i}{3}\right)\mathbb{E}_L + 2\left(k_i + \frac{\mu_i}{3}\right)\mathbb{J}_T + \sqrt{2}\left(k_i - \frac{2\mu_i}{3}\right)\left({}^{\mathsf{T}}\mathbb{F} + \mathbb{F}\right) + 2\mu_i\left(\mathbb{K}_T + \mathbb{K}_L\right) \\ \mathbb{P}_1 &= \frac{3}{2\left(3k_1+4\mu_1\right)}\mathbb{J}_T + \frac{1}{4\mu_1}\frac{3k_1+7\mu_1}{3k_1+4\mu_1}\mathbb{K}_T + \frac{1}{4\mu_1}\mathbb{K}_L \end{aligned}\right\} \quad \text{for cylindrical inclusions} \tag{5}$$

where k_i and μ_i are the bulk and the shear modulus respectively of the phase i, $\mathbb{J} = (1/3)\boldsymbol{i}\otimes\boldsymbol{i}$ and $\mathbb{K} = \mathbb{I} - \mathbb{J}$, $\boldsymbol{i}$ being the identity of second-order tensors, $\boldsymbol{i}_T = \boldsymbol{i} - \boldsymbol{n}\otimes\boldsymbol{n}$, $\mathbb{E}_L = \boldsymbol{n}\otimes\boldsymbol{n}\otimes\boldsymbol{n}\otimes\boldsymbol{n}$, $\mathbb{J}_T = (1/2)\boldsymbol{i}_T\otimes\boldsymbol{i}_T$, $\mathbb{F} = (1/\sqrt{2})\boldsymbol{n}\otimes\boldsymbol{n}\otimes\boldsymbol{i}_T$, $\mathbb{K}_T = \mathbb{I}_T - \mathbb{J}_T$, $\mathbb{K}_L = 2[\boldsymbol{n}\otimes\boldsymbol{i}_T\otimes\boldsymbol{n}]^{(S)}$, $\boldsymbol{n}$ is the out-of-plane unit vector, $\boldsymbol{i}_T$ is the identity of second-order tensors in the transverse plane.

In the case of elastic inclusions ($k_2 > 0$, $\mu_2 > 0$), the bulk and shear moduli of the unknown phase are obtained as roots of a system of two equations (6) or (7) depending on the considerate case. The left hand terms of these equations are determined with the help of field measurements and the right hand terms depend only on the mechanical properties of two phases. If the properties of the phase 1 (resp. 2) are supposed to be known, the unknowns are the properties of the phase 2 (resp. 1).

$$\left.\begin{aligned} \frac{\langle\boldsymbol{\varepsilon}\rangle_1 : \mathbb{J} : \langle\boldsymbol{\varepsilon}\rangle_1}{\boldsymbol{\varepsilon}^{\text{hom}} : \mathbb{J} : \boldsymbol{\varepsilon}^{\text{hom}}} &= \left(\frac{4\mu_1 + 3k_2}{3f_2k_1 + 4\mu_1 + 3\left(1-f_2\right)k_2}\right)^2 \\ \frac{\langle\boldsymbol{\varepsilon}\rangle_1 : \mathbb{K} : \langle\boldsymbol{\varepsilon}\rangle_1}{\boldsymbol{\varepsilon}^{\text{hom}} : \mathbb{K} : \boldsymbol{\varepsilon}^{\text{hom}}} &= \left(\frac{\mu_1\left(9k_1+8\mu_1\right) + 6\mu_2\left(k_1+2\mu_1\right)}{\mu_1\left(9k_1+8\mu_1\right) + 6\left(\mu_2 + f_2\left(\mu_1-\mu_2\right)\right)\left(k_1+2\mu_1\right)}\right)^2 \end{aligned}\right\} \quad \text{for spherical inclusions} \tag{6}$$

$$\left.\begin{aligned} \frac{\langle\boldsymbol{\varepsilon}\rangle_1 : \mathbb{J}_T : \langle\boldsymbol{\varepsilon}\rangle_1}{\boldsymbol{\varepsilon}^{\text{hom}} : \mathbb{J}_T : \boldsymbol{\varepsilon}^{\text{hom}}} &= \left(\frac{3\mu_1 + 3k_2 + \mu_2}{3f_2k_1 + \left(3+f_2\right)\mu_1 + \left(1-f_2\right)\left(3k_2+\mu_2\right)}\right)^2 \\ \frac{\langle\boldsymbol{\varepsilon}\rangle_1 : \mathbb{K}_T : \langle\boldsymbol{\varepsilon}\rangle_1}{\boldsymbol{\varepsilon}^{\text{hom}} : \mathbb{K}_T : \boldsymbol{\varepsilon}^{\text{hom}}} &= \left(\frac{\mu_1\left(3k_1+\mu_1\right) + \mu_2\left(3k_1+7\mu_1\right)}{\mu_1\left[f_2\left(3k_1+7\mu_1\right) + 3k_1 + \mu_1\right] + \mu_2\left(1-f_2\right)\left(3k_1+7\mu_1\right)}\right)^2 \end{aligned}\right\} \quad \text{for cylindrical inclusions} \tag{7}$$

In the case of porous inclusions ($k_2 = 0$, $\mu_2 = 0$), the previous systems lead to a vanishing determinant (the strain concentration tensor of the pore phase $\mathbb{A}_2$ is not defined) and additional informations are required to identify the matrix properties (k_1, μ_1). Since, overall stress-strain relationship is known at the scale of the sample, the overall Young's modulus E^{hom} can be identified. In addition, overall in-plane strain field allow to determine the overall Poisson's ratio ν^{hom}. The matrix properties are thus obtained as:

$$\left.\begin{aligned} &\bullet\ \text{Spherical inclusions:} \quad k_1 = \frac{E^{\text{hom}}}{2\left(1+\nu^{\text{hom}}\right)}\frac{9+6f_2+\left(8+12f_2\right)\mathcal{A}}{f_1\mathcal{A}\left(9+8\mathcal{A}\right)}, \quad \mu_1 = \mathcal{A}k_1 \\ &\mathcal{A} = \frac{3k_1}{16(\nu^{\text{hom}}+1)}\Big(\sqrt{\left(196f_2^2+220f_2+25\right)\left(\nu^{\text{hom}}\right)^2 - \left(112f_2^2+196f_2+70\right)\nu^{\text{hom}} + 16f_2^2+16f_2+49} \\ &\qquad\qquad + 4f_2 - 11\nu^{\text{hom}} - 14f_2\nu^{\text{hom}} + 1\Big) \end{aligned}\right\} \tag{8}$$

$$\bullet\ \text{Cylindrical inclusions:} \quad k_1 = \frac{E^{\text{hom}}}{2\left(1+\nu^{\text{hom}}\right)}\frac{3+\mathcal{B}+f_2\left(3+7\mathcal{B}\right)}{f_1B\left(3+\mathcal{B}\right)}, \quad \mu_1 = \mathcal{B}k_1, \quad \mathcal{B} = \frac{3}{2}\frac{2\nu^{\text{hom}}\left(1+f_2\right)-1}{3f_2-1-\nu^{\text{hom}}\left(1+7f_2\right)} \tag{9}$$

3. ACCURACY OF THE APPROACH: NUMERICAL DATA

First, the accuracy of the approach (equations (6)-(7) for elastic inclusions or (8)-(9) for voids) is verified on numerical simulations (CAST3M): a single inclusion is embedded in a matrix with remote loading. These numerical simulations have two main interests: 1/ at finite element convergence, the stress and strain fields are determined without noise, 2/ as far as the volume fraction of inclusion remains small, the considered microstructure corresponds to the Eshelby's problem for which equations (4) and (5) are rigorous. The volume fraction of inclusion f_2 below which this last condition is satisfied is estimated using a criterion on the intraphase homogeneity inside the inclusion: the ratio of standard deviation of the strain field on its mean has to be less than 10^{-1}. For elastic inclusions, this criterion leads to $f_2 \leq 20\%$ (this criterion is plotted in black in Figure 1 without units). We assume that the same value is still valid for porous inclusions.

The results are given in Figure 1: the relative errors on estimated moduli (by comparison to the values employed for performing the numerical simulations) are given as a function of the volume fraction of the inclusions. For elastic inclusions, if the properties of the matrix (resp. the inclusions) are supposed to be known, the properties of the inclusions (resp. the matrix) are identified, Figure 1 (b-c). For porous inclusions, only the properties of the matrix are identified, Figure 1 (e-f). For spherical inclusions, the approach leads to an error less than about 10%, Figure 1 (b-e). For cylindrical inclusions, the error is less than about 5%, Figure 1 (c-f). We have a decline that the mechanical contrast between each phase is about 4 in this test ($k_2/k_1 = \mu_2/\mu_1 \simeq 4$). In the physical situation that we have in mind, the contrast is much lower than this value and the phase that should be identified is the inclusion phase. For a volume fraction of inclusions lower than 20%, the expected relative error in such a 'perfect case' is thus lower than 5%.

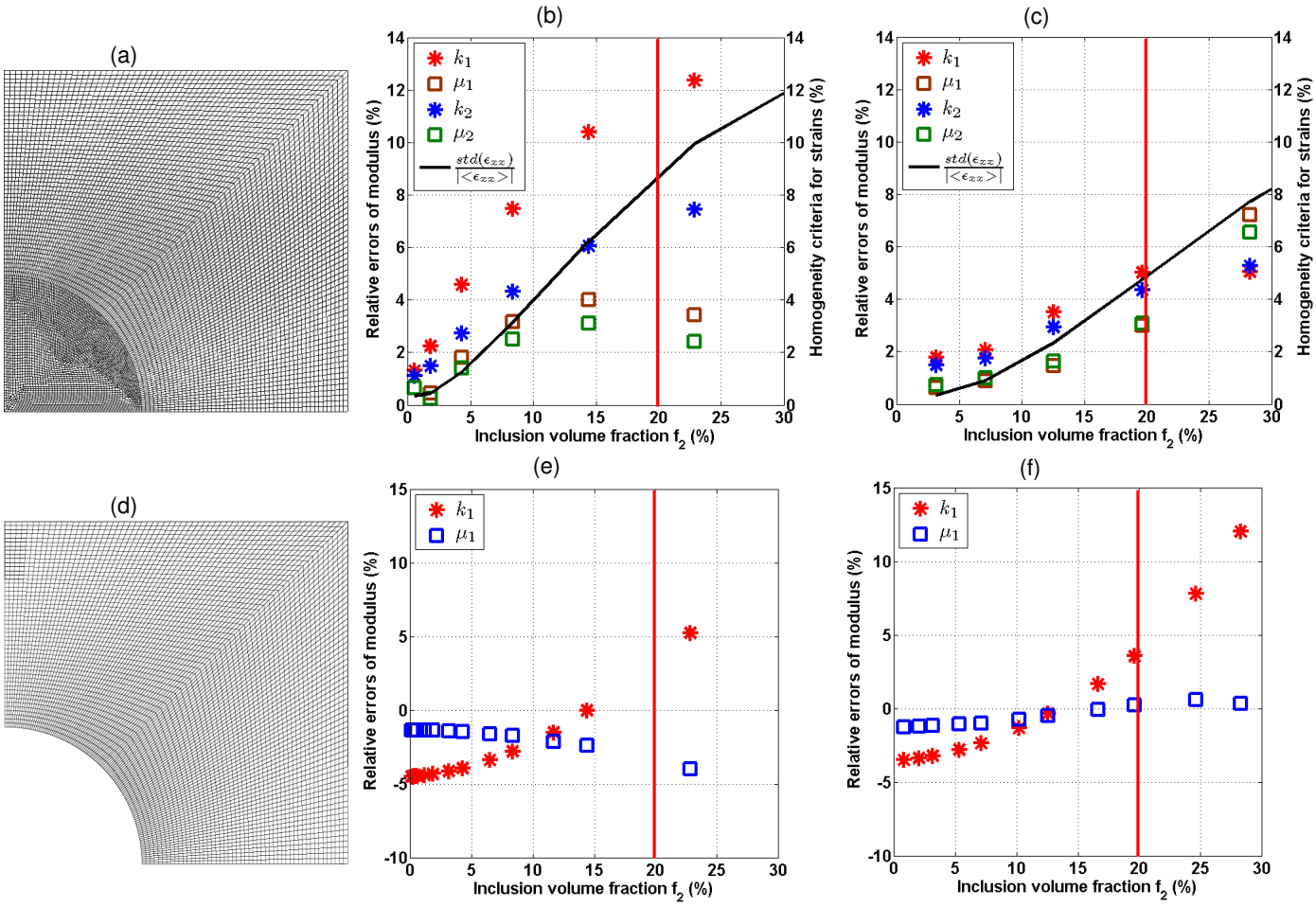

Figure 1 - Mesh 2D models used in CAST3M simulation for (spherical or cylindrical) elastic inclusion material (a) and (spherical or cylindrical) porous inclusion material (d). Relative errors for the identified bulk and shear moduli using virtual fields obtained by numerical simulations: (b) spherical elastic inclusion material; (c) cylindrical elastic inclusion material; (e) spherical porous inclusion material; (f) cylindrical porous inclusion material

4. ACCURACY OF THE APPROACH: EXPERIMENTAL DATA

We consider uniaxial tensile tests for two types of samples: a unique cylindrical void and four cylindrical voids arranged in a square pattern embedded in an elasto-plastic matrix. The matrix is a recrystallized annealed (RXA) Zircaloy-4. Samples are thin plate specimens of 435μm initial thickness. The diameter of the voids is about 90μm (made by electrical discharge machining). The length-to-diameter ratio of the voids is thus about 5, therefore, the mechanical states are complex around the voids: plane strain near the void, plane stress away from the void.

The elastic properties k_1 and μ_1 of the matrix are determined experimentally from a uniaxial tensile test on a homogeneous sample. For the voided samples, the relative errors on the estimated values of k_1 and μ_1 are given in Figure 2 (d-e) as a function of the overall uniaxial applied strain $\varepsilon_{yy}^{\text{hom}}$. For low values of $\varepsilon_{yy}^{\text{hom}}$, typically below about 0.1%, the DIC technique concerning our device reaches its limits of sensitivity. For higher values or $\varepsilon_{yy}^{\text{hom}}$, typically above about 0.3%, some local plasticity develops near the voids. As expected, this plasticity appears for lower applied strain in the case of four voids (interaction between voids). Within this strain domain, the proposed inverse approach is valid and less than $10-12\%$ relative error is obtained. In comparison to the 'perfect' numerical case, no significant effect due to the experimental noise is noticed.

5. IDENTIFICATION OF THE PROPERTIES OF AN α-PHASE IN AN HETEROGENEOUS OXIDIZED ZIRCALOY

An oxidized RXA Zircaloy-4 plate is now investigated. The microstructure of this heterogeneous material is made of α-phase inclusions and a β-phase matrix. The sample preparation process includes a long term high temperature annealing step, leading to oxygen concentrations that are homogeneous within each phase. Mechanical properties of each phase are thus supposed to be homogeneous and to have values reported in the literature [1]. Compared to the previous cases, a higher volume fraction of inclusions (about 40%) is considered, the inclusions have whiskers-type shapes and the isotropy of the spatial distribution of the phases is not fully controlled. These parameters have a significant influence on the precision of estimated properties of the inclusion phase and more inaccuracy is expected. The Figure 2 (f) show an important error for the estimated bulk modulus, but the estimated shear modulus is quite accurate. We recall that these relative errors are given by comparison to results previously reported in the literature [1].

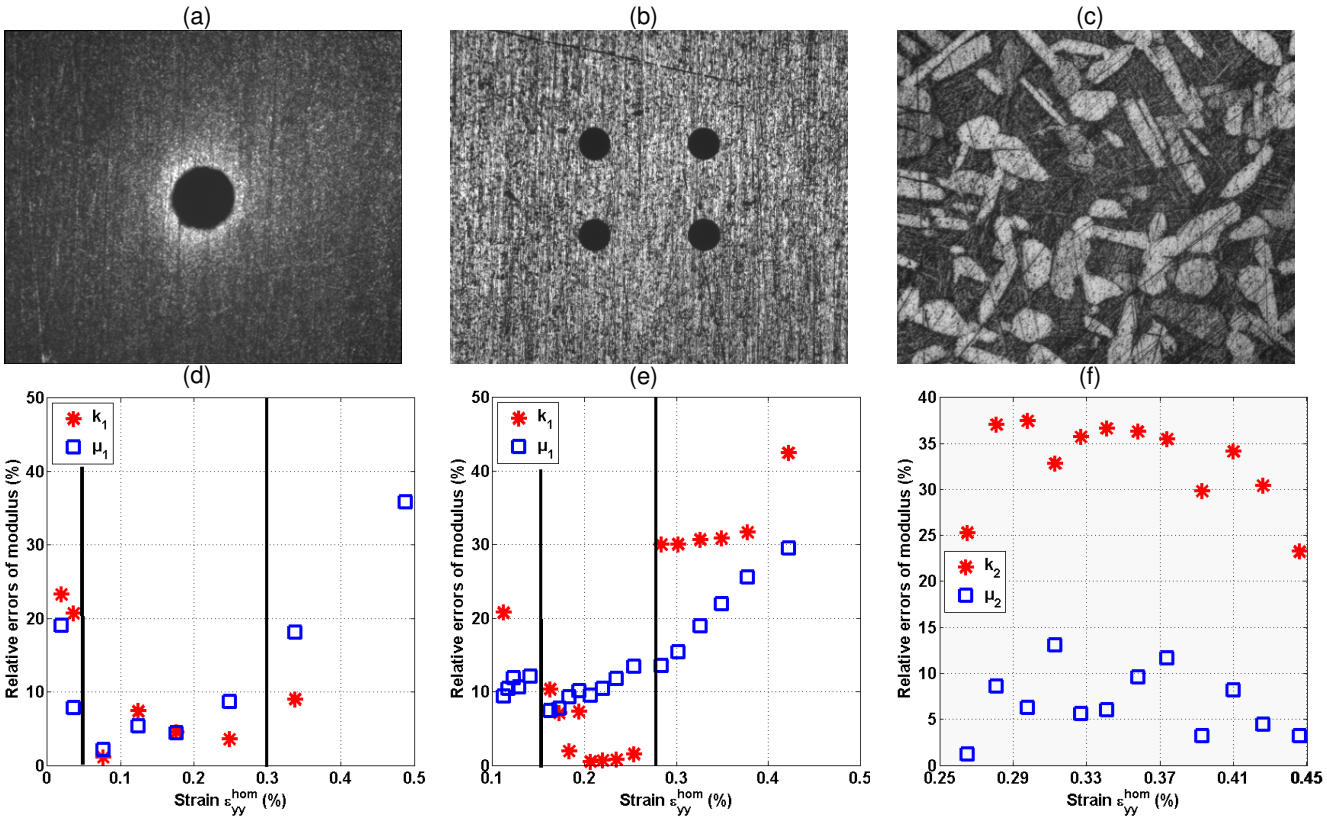

Figure 2 - Microstructure of test specimen surface obtained by a long-focal-length microscope: (a) a single cylindrical void sample (590 x 494 pixels); (b) four cylindrical voids sample (1064 x 891 pixels); (c) oxidized Zircaloy-4 sample (590 x 494 pixels). Relative errors for the identified bulk and shear moduli obtained by the inverse homogenization method coupled with DIC field measurements: (d) properties of the matrix phase containing a single cylindrical void; (e) properties of the matrix phase containing four cylindrical voids; (f) properties of the α-phase (inclusions) in an oxidized Zircaloy-4 sample.

6. CONCLUSIONS

This paper presents an approach for experimental identification of linear elastic properties of each phase in an heterogeneous material. This approach rests on an inverse identification coupling an homogenization scheme and full-field measurement based on digital image correlation. The proposed methodology concerns heterogeneities whose characterized size is about few tens of microns. The accuracy of the approach was estimated: 1/ on virtual fields obtained by numerical simulations, 2/ on real fields obtained for porous materials with design microstructures. The ranges of validity of the method were characterized. Within these ranges, the accuracy of the method is about 10%. The method was tested far outside these ranges on an oxidized Zircaloy-4 material. The shear (resp. bulk) modulus of an α-phase was identified with an accuracy of 10% (resp. 30%). These results have to be confirmed on controlled microstructures and extended to plastic behaviours.

7. REFERENCES

1. Stern A. (2001) Comportements métallurgique et mécanique des matériaux de gainage du combustible REP oxydés à haute température. *Phd thesis*, Ecole des Mines de Paris
2. Wattrisse B. (1999) Etude cinématique des phénomènes de localisation dans un acier par intercorrélation d'images. *Phd thesis*, Université Montpellier II
3. El Bartali A. (2007) Apport de mesures de champs cinématiques à l'étude des micromécanismes d'endommagement en fatigue plastique d'un acier inoxydable duplex. *Phd thesis*,Ecole Centrale de Lille
4. Vander Voort G.F. (1984) Metallography, principles and practice. *ASM International*
5. Ma L., Chen Y.Q., Moore K. (2004) Rational radial distortion models of camera lenses with analytical solution for distortion correction. *International Journal of Information Acquisition*, 1, 2, 135-147
6. Bornert M., Bretheau T., Gilormini P. (2001) Homogénéisation en mécanique des matériaux 1: Matériaux aléatoires élastiques et milieux périodiques (Traité MIM, série alliages métalliques). *Hermes Science, Paris*
7. Hill R. (1965) Continuum micro-mechanics of elastoplastic polycrystals. *Journal of the Mechanics and Physics of Solids*, 13, 2, 89-101
8. Mura, T. (1991) Micromechanics of defects in solids, Kluwer Academic Publisher